On the Amplify-and-Forward Cooperative Diversity with Time-Hopping Ultra-Wideband Communications

Chadi Abou-Rjeily, *Member IEEE*, Norbert Daniele and Jean-Claude Belfiore, *Member IEEE*

***Abstract*— In this paper, we extend the Amplify-and-Forward cooperative diversity scheme to the context of impulse radio ultra wideband (IR-UWB). In particular, we present the construction of three families of minimal-delay and totally-real distributed algebraic space-time (ST) codes suitable for IR-UWB. The first family encodes adjacent symbols and is based on totally-real cyclic division algebras. The second family encodes the pulses used to transmit one information symbol and permits to achieve high performance levels with lower complexity. Both families of codes achieve full rate, full diversity with non-vanishing determinants for various number of relays. These schemes can be associated with pulse position modulation (PPM), pulse amplitude modulation (PAM) and hybrid pulse position and amplitude modulation (PPM-PAM). The third family of codes is information-lossless and does not require any pulse repetitions. It is specific to M-PPM-M'-PAM with $M \geq 3$ and for all values of M'. Simulations performed over realistic indoor UWB channels are provided to verify the theoretical results.**

***Index Terms*— Time Hopping Ultra-Wideband (TH-UWB), cooperative diversity, Space Time (ST), Pulse Amplitude Modulation (PAM), Pulse Position Modulation (PPM), Rake, Non-Vanishing Determinant (NVD).**

I. Introduction

The attractive features of ultra-wideband (UWB) communication systems make them strong candidates for short-range high-rate applications. However, the low tolerated transmission levels [1] and the propagation properties of the UWB signals can become a limiting factor on the performance. The utility of spatial diversity with UWB systems was outlined in different contributions [2]–[4]. Despite the high frequency selectivity of the UWB channels, profiting from the multi-path diversity can necessitate Rake receivers with very high orders. This follows from the very important delay spread of these channels. Moreover, UWB channels are subject to cluster fading where it is not improbable that a large number of consecutive multi-path components have small amplitudes (interested readers may refer to [5], [6] for more details on the nature of fading in UWB channels). In this context, the additional spatial degree of freedom can result in higher performance levels, multiplexing gains and communication ranges. On the other hand, for most ad hoc and sensor networks, a limited number of antennas can be deployed at each radio terminal. In this context, the cooperative diversity techniques can be beneficial where the spatial diversity is exploited in a distributed manner among the different terminals [7]–[10]. However, these schemes were investigated uniquely in the narrow band and wideband context.

Among the different cooperation strategies, the nonorthogonal amplify-and-forward (NAF) scheme was shown to have the best diversity-multiplexing tradeoff among all previously proposed AF schemes [9]. Explicit algebraic constructions of short block codes based on the NAF scheme were proposed in [10]. However, these complex-valued codes are not adapted to real carrier-less impulse radio UWB. In fact, phase rotations applied to the very short pulses are infeasible given the very large bandwidth occupied by these pulses. Apart from this limiting constraint, time-hopping (TH) UWB has an appealing feature that resides in the transmission of a train of pulses for conveying one information symbol. As shown later, this additional degree of freedom can be beneficial in enhancing the system performance and simplifying the receiver structure.

The first main contribution of this paper is the extension of the complex-valued codes presented in [10] to real carrier-less UWB transmissions. Totally-real cyclic division algebras [11] with real "non-norm" algebraic elements result in full rate, full diversity and minimal delay codes with non-vanishing coding gains for a wide range of the number of cooperating relays. However this construction presents two disadvantages which follow from the constraint of having totally-real codewords. The first one is that the transmitted energy is not uniformly distributed among the different components of the codewords. The second disadvantage follows, as shown later, from the non-existence of totally-real information-lossless codes based on cyclic division algebras.

In order to overcome the first disadvantage, the pulse repetitions (when present) are exploited in order to balance the proposed codewords resulting in better performance and a better distribution of the error events among the different symbols. Moreover, a second family of UWB-specific codes is proposed and shown to be the optimal extension of the first family of codes when inter pulse coding (IPC) is performed.

The second main contribution consists of overcoming the second disadvantage by proposing a new family of codes that is not based on cyclic division algebras. Instead of adopting the "classical" approach of constructing codes over the hypercubes carved from the lattice of rational integers [10], [12], we

C. Abou-Rjeily is with the Department of Electrical and Computer Engineering, Lebanese American University (LAU), P.O.B. 36 Byblos, Lebanon. (e-mail: chadi.abourjeily@lau.edu.lb).

N. Daniele is with the Laboratory of Electronics and Information Technology (LETI), Atomic Energy Commission (CEA), 17 rue des Martyrs, 38054 Grenoble, France. (e-mail: norbert.daniele@cea.fr).

J.-C. Belfiore is with the COMELEC department, École Nationale Supérieure des Télécommunications (ENST), 46 rue Barrault 75013 Paris, France. (e-mail: belfiore@enst.fr).

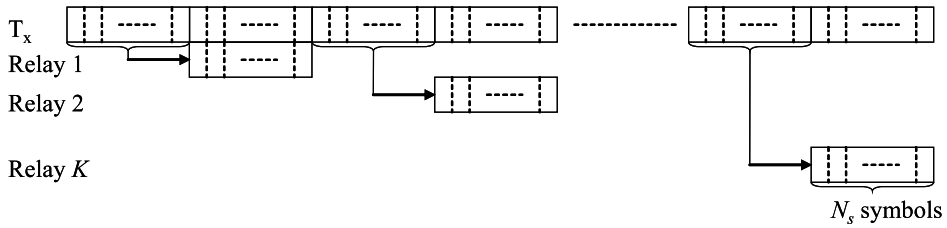

Fig. 1. The NAF protocol with K relays.

exploited the structure of M-PPM-M'-PAM constellations in order to construct an information-lossless code. Unlike the first two families of codes, this construction is specific to M-PPM-M'-PAM for $M \geq 3$ and for all values of M'. For these modulations, this approach shows the best performance among systems that do not use pulse repetitions. The performance of the constructed codes is investigated over realistic indoor UWB channels [5], [13], [14] and Rake receivers are implemented at the cooperating relays and the receiver.

Notations: I_n and $\mathbf{0}_n$ correspond to the $n \times n$ identity matrix and the all-zero matrix respectively. $1_{m\times n}$ and $\mathbf{0}_{m\times n}$ are the $m \times n$ matrices whose elements are equal to 1 and 0 respectively. $*$ and $\otimes$ stand for convolution and the Kronecker product respectively. $\det(X)$ is the determinant of matrix X. The function $\text{diag}(X_1, ..., X_n)$ stacks the corresponding matrices on the principal diagonal. The function $\text{vec}(X)$ stacks the columns of matrix X vertically one after the other. $\mathbb{Q}$ denotes the field of rational numbers while the function $\text{N}_{\mathbb{K}/\mathbb{Q}}(x)$ corresponds to the algebraic norm of the element x in the field extension $\mathbb{K}/\mathbb{Q}$.

II. System model

Consider the case of a wireless network consisting of a certain number of synchronous half-duplex radio terminals each equipped with a single antenna. We consider the case where K neighboring terminals (relays) can help the source in delivering its message to a given destination. During the cooperative mode, the K nodes will share the same time hopping sequence as the source. In what follows, we differentiate between PAM and PPM-PAM constellations.

A. PAM constellations

Consider the NAF scheme proposed in [9] and described in Fig. 1. For this protocol, each relay enters in cooperation with the source during a period of $2N_s$ symbol durations. The N_s symbols received during the first half of this cooperation period are amplified and retransmitted by the cooperating relay during the second half. In what follows, $\mathcal{A}_{k,1}$ and $\mathcal{A}_{k,2}$ are $1 \times N_s$ matrices. $\mathcal{A}_{k,i}$ is transmitted during the i-th half of the k-th cooperation interval for $i = 1, 2$ and $k = 1, \ldots, K$. These matrices are given by: $\mathcal{A}_{k,1} = [A_{2(k-1)N_s+1} \ \cdots \ A_{(2k-1)N_s}]$ and $\mathcal{A}_{k,2} = [A_{(2k-1)N_s+1} \ \cdots \ A_{2kN_s}]$ where $A_j \in \{2m' - 1 - M'; m' = 1, \ldots, M'\}$ is the j-th information symbol that belongs to the M'-ary PAM constellation.

In TH-UWB communications, several time hopped pulses are used for the transmission of one information symbol. In addition to this TH sequence, we also introduce an additional amplitude spreading sequence. At the end of this section, we will see that this additional spreading can enhance the performance of cooperative systems. Designate by N_f the number of pulses per symbol. The $1 \times N_f$ amplitude spreading vectors corresponding to A_j will be denoted by B_1 and B_2 for $j = 2(k-1)N_s+1, \ldots, (2k-1)N_s$ and $j = (2k-1)N_s + 1, \ldots, 2kN_s$ respectively and for $k = 1, \ldots, K$.

We consider the case where the relays and the destination are equipped with L-th order Rakes. In the absence of inter-symbol-interference (ISI) and multi-user-interference (MUI), the TH sequence has no impact on the system performance. In this case, the decision variables collected at the k-th relay during the first half of the k-th cooperation period can be expressed as:

$$X_k = \sqrt{\frac{\beta_1 \rho_k}{N_f}} H_k \left(\mathcal{A}_{k,1} \otimes B_1\right) + N'_k \tag{1}$$

where the decision variables and the noise terms are included in the $(L \times N_s N_f)$-dimensional matrices X_k and N'_k respectively. ρ_k is the path-loss term corresponding to the relative quality of the channel between the source and the k-th relay with respect to the channel between the source and the destination ($\rho_0 = 1$). When transmitting during the first half of each one of the K cooperation periods, the energy transmitted by the source is scaled by β_1. H_k is a L-dimensional vector that corresponds to the channel between the source and the k-th relay. The l-th element of H_k corresponds to the impact of the transmitted signal on the l-th Rake finger of the k-th relay. This term is given by: $H_{k,l} = h_k(\Delta_l)$ where Δ_l is the l-th finger delay and h_k corresponds to the frequency selective channel between the transmitter and the k-th relay [3].

As in eq. (1), the decision variables collected at the destination during the first half of the k-th cooperation period can be expressed as:

$$Y_{k,1} = \sqrt{\frac{\beta_1}{N_f}} H_0 \left(\mathcal{A}_{k,1} \otimes B_1\right) + N_{k,1} \tag{2}$$

where H_0 is the vector associated with the channel from the source to the destination.

A simple AF strategy at each relay will result in a received signal (at the destination) that has an excessively big channel delay spread (twice that of the UWB channels). This implies two major inconveniences. In order to eliminate the ISI, the symbol durations must be increased resulting in lower data rates. On the other hand, higher order Rake receivers must be implemented at the destination since the energy collected

by each finger is now very small. In order to overcome these limitations, we chose to perform maximum-ratio-combining (MRC) prior to amplification and retransmission. In other words, the signal transmitted from the k-th relay during the second half of the k-th cooperation period is given by:

$$X'_k = \sqrt{\beta_2}\Psi_k H_k^T X_k \tag{3}$$

where Ψ_k is the amplification factor given by:

$$\Psi_k = \left(H_k^T H_k\right)^{-\frac{1}{2}} \left(\beta_1 \rho_k H_k^T H_k + \frac{N_0}{2}\right)^{-\frac{1}{2}} \tag{4}$$

where $N_0/2$ is the double sided spectral density of the additive white Gaussian noise.

When transmitting simultaneously during the second half of the k-th cooperation period, the k-th relay and the source are supposed to the have the same transmission levels (determined by β_2) for $k = 1, \ldots, K$. Transmitting the same energy as in non-cooperative systems corresponds to fixing $\beta_1 + 2\beta_2 = 2$.

Replacing eq. (1) in eq. (3) results in:

$$X'_k = \sqrt{\frac{\beta_1\beta_2\rho_k}{N_f}}\Psi_k H_k^T H_k(\mathcal{A}_{k,1} \otimes B_1) + \sqrt{\beta_2}\Psi_k H_k^T N'_k \tag{5}$$

Finally, the decision matrix at the destination during the second half of the k-th cooperation period can be expressed as:

$$Y_{k,2} = \sqrt{\frac{\beta_2}{N_f}} H_0 \left(\mathcal{A}_{k,2} \otimes B_2\right) + \sqrt{\lambda_k} G_k X'_k + N_{k,2} \tag{6}$$

where λ_k is determined in a similar way as ρ_k and it stands for the quality of the channel between the k-th relay and the destination. G_k is a L-dimensional vector that stands for the channel between the k-th relay and the destination.

Replacing the value of X'_k (given in eq. (5)) in eq. (6), the decision variables collected at the destination during the k-th cooperation period can be expressed as:

$$\begin{bmatrix} Y_{k,1} \\ Y_{k,2} \end{bmatrix} = \begin{bmatrix} \sqrt{\beta_1} H_0 & \mathbf{0}_{L\times 1} \\ \sqrt{\beta_1\beta_2\rho_k\lambda_k} G_k \Psi_k H_k^T H_k & \sqrt{\beta_2} H_0 \end{bmatrix} \begin{bmatrix} \mathcal{A}_{k,1} \otimes B_1 \\ \mathcal{A}_{k,2} \otimes B_2 \end{bmatrix} + \mathcal{N}_k \tag{7}$$

where the factor N_f was removed from the expression of the channel matrix and included in the noise variance. The noise matrix can be written as $\mathcal{N}_k = [\mathcal{N}_{k,1}^T \;\; \mathcal{N}_{k,2}^T]^T$. $\mathcal{N}_{k,1}$ is equal to the matrix $N_{k,1}$ given in eq. (2). From equations (5) and (6): $\mathcal{N}_{k,2} = \sqrt{\beta_2\lambda_k} G_k \Psi_k H_k^T N'_K + N_{k,2}$.

After noise whitening, eq. (7) can be written as:

$$Y_k = \widetilde{H}_k \begin{bmatrix} \mathcal{A}_{k,1} \otimes B_1 \\ \mathcal{A}_{k,2} \otimes B_2 \end{bmatrix} + N_k \tag{8}$$

where N_k is white and the matrix $\widetilde{H}_k$ is given by:

$$\widetilde{H}_k \triangleq \begin{bmatrix} \sqrt{\beta_1} H_0 & \mathbf{0}_{L\times 1} \\ \sqrt{\beta_1\beta_2\rho_k\lambda_k}\Sigma_k^{-\frac{1}{2}} G_k \Psi_k H_k^T H_k & \sqrt{\beta_2}\Sigma_k^{-\frac{1}{2}} H_0 \end{bmatrix} \tag{9}$$

where the noise whitening matrix was determined from:

$$\Sigma_k = I_L + \beta_2\lambda_k\Psi_k^2 (H_k^T H_k) G_k G_k^T \tag{10}$$

Stacking the decision matrices corresponding to the K different cooperation intervals horizontally, we obtain the following relation:

$$Y_{(2L\times KN_sN_f)} = \tilde{H}_{(2L\times 2K)} \mathcal{A}_{(2K\times KN_sN_f)} + N_{(2L\times KN_sN_f)} \tag{11}$$

where the subscripts indicate the corresponding matrices' dimensions. Y, $\tilde{H}$ and N are obtained by stacking the matrices Y_k, $\tilde{H}_k$ and N_k horizontally for $k = 1, \ldots, K$. $\mathcal{A}$ is given by:

$$\mathcal{A} = \text{diag}\left(\begin{bmatrix} \mathcal{A}_{1,1} \otimes B_1 \\ \mathcal{A}_{1,2} \otimes B_2 \end{bmatrix} \quad \cdots \quad \begin{bmatrix} \mathcal{A}_{K,1} \otimes B_1 \\ \mathcal{A}_{K,2} \otimes B_2 \end{bmatrix} \right) \tag{12}$$

The encoding scheme is determined from the choice of the matrix $\mathcal{A}$.

B. Hybrid PPM-PAM constellations

We now consider hybrid M-PPM-M'-PAM constellations where each modulated pulse can occupy M positions with an amplitude that can take M' possible values. This is a M-dimensional constellation where each information symbol is represented by a M-dimensional vector belonging to the set:

$$\mathcal{C} = \left\{(2m' - 1 - M')e_m^T \;;\; m' = 1, \ldots, M';\; m = 1, \ldots, M\right\} \tag{13}$$

where e_m stands for the m-th row of the $M \times M$ identity matrix I_M.

In this case, being sequences of N_s information symbols, $\mathcal{A}_{k,1}$ and $\mathcal{A}_{k,2}$ will now become $(M \times N_s)$-dimensional matrices where the j-th column of $\mathcal{A}_{k,i}$ stands for the vector representation of the symbol transmitted during the j-th symbol duration of the i-th half of the k-th cooperation period for $j = 1, \ldots, N_s$, $i = 1, 2$ and $k = 1, \ldots, K$.

The same formulation will hold as in the case of PAM. However, the different channel matrices H_0, H_k and G_k will become $LM \times M$ matrices (rather than L-dimensional vectors). In this case, the $((l-1)L + m, m')$-th element of each channel matrix corresponds to the impact of the signal transmitted during the m'-th position on the m-th correlator (corresponding to the m-th position) placed after the l-th Rake arm for $l = 1, \ldots, L$ and $m, m' = 1, \ldots, M$. Consequently, LM decision variables are collected for the detection of one pulse resulting in LMN_sN_f decision variables collected during one half of each cooperation period. In other words, the decision matrices X_k and $Y_{k,1}$ given in eq. (1) and eq. (2) will become $LM \times N_sN_f$ matrices.

Given that each pulse can now occupy M positions, then the amplification factor Ψ_k given in eq. (4) will now become an amplification matrix that takes the following form:

$$\Psi_k = \left(H_k^T H_k\right)^{-\frac{1}{2}} \left(\beta_1 \rho_k H_k^T H_k + \frac{N_0}{2} I_M\right)^{-\frac{1}{2}} \tag{14}$$

As a conclusion, the input-output relation given in eq. (8) will always hold for M-dimensional constellations. Given that all the channel matrices will have dimensions $LM \times M$, the sub-matrix on the first row and second column of $\tilde{H}_k$ must be equal to $\mathbf{0}_{LM\times M}$.

Finally, given the new dimensionality of the channel matrices and the amplification matrix Ψ_k, the noise whitening matrix must not be determined from eq. (8) but from:

$$\Sigma_k = I_{LM} + \beta_2 \delta_k G_k \Psi_k H_k^T H_k \Psi_k^T G_k^T \tag{15}$$

III. Distributed ST codes with PAM

In this section, we consider the code construction with PAM constellations. Distributed ST coding with hybrid PPM-PAM constellations will be considered in section IV. For PAM, we propose two families of codes that are based on totally-real cyclic division algebras. In particular, we distinguish between Inter Symbol Coding (ISC) and Inter Pulse Coding (IPC). The first scheme encodes adjacent symbols while the second scheme encodes the pulses used to convey one information symbol.

A. Inter Symbol Coding (ISC)

In this case $B_1 = B_2 = B = 1_{1\times N_f}$. Since this encoding scheme is independent from the pulse repetitions, then it can be applied even in the absence of these repetitions (when $N_f = 1$). Equation (12) can be expressed as: $\mathcal{A} = C \otimes B$ where C is the $2K \times KN_s$ matrix corresponding to the distributed space time coding scheme. It is given by:

$$C = \text{diag}\left(C_1, ..., C_K\right) \tag{16}$$

$$C_k = \begin{bmatrix} A_{k,1}^T & A_{k,2}^T \end{bmatrix}^T \tag{17}$$

note that C_k is a $2 \times N_s$ matrix for $k = 1, ..., K$.

From eq. (11), combining the decision variables corresponding to the different pulses of the same symbol is equivalent to calculating:

$$\begin{aligned} Y\left(I_{KN_s} \otimes B^T\right) &= \tilde{H}\left(C \otimes B\right)\left(I_{KN_s} \otimes B^T\right) + N & (18)\\ &= N_f \tilde{H} C + N & (19)\end{aligned}$$

where it is easy to verify that the noise term is still white (with variance $\frac{N_f^2 N_0}{2}$).

Since C_k is a $2\times N_s$ matrix, it can be directly seen that there is no interest in choosing $N_s > 2$. Therefore, in what follows we fix $N_s = 2$ resulting in minimal-delay codes. Moreover, in order to achieve full rate, $2N_sK$ symbols must be included in each codeword C. Furthermore, in order to achieve full diversity, all of these $4K$ symbols must be included in the sub-matrices C_k for all values of k.

For the construction of C, we use the approach proposed in [10] where the distributed codes were constructed based on cyclic division algebras [11], [12]. As mentioned earlier, these complex-valued constructions are not suitable for real carrier-less UWB transmissions. Therefore, in what follows we extend the family of codes proposed in [10] to UWB communications by performing the construction in totally-real field extensions.

Let $\mathbb{K} = \mathbb{Q}(\theta)$ and $\mathbb{F} = \mathbb{Q}(\phi)$ be the K and 2 dimensional real cyclic field extensions of $\mathbb{Q}$ respectively where θ is a real number and $\phi = \frac{1+\sqrt{5}}{2}$ is the golden number. Their Galois groups are given by $Gal(\mathbb{K}/\mathbb{Q}) = \langle\sigma\rangle$ (with $\sigma^K = 1$) and $Gal(\mathbb{F}/\mathbb{Q}) = \langle\tau\rangle$ (with $\tau^2 = 1$). In the same way, we define $\mathbb{L} = \mathbb{Q}(\theta, \phi)$ a cyclic extension of $\mathbb{K}$ with degree 2.

At a second time we construct the cyclic algebra $\mathcal{A} = (\mathbb{L}/\mathbb{K}, \tau, \gamma)$. As a reminder about the construction of codes based on cyclic algebras, we recall that $\mathcal{A}$ can be decomposed as $\mathcal{A} = \mathbb{L} \oplus z\mathbb{L} \oplus \cdots \oplus z^{n-1}\mathbb{L}$ where $z \in \mathcal{A}$ verifies $lz = z\tau(l)$ for all $l \in \mathbb{L}$ and $l^n = \gamma \in \mathbb{K}$ where $n = 2$ is the degree of $\mathbb{L}/\mathbb{K}$ (interested readers may refer to [10], [11] for more details). In matrix representation, elements of $\mathcal{A}$ can be represented by:

$$C_0 = \begin{bmatrix} l_1 & l_2 \\ \gamma\tau(l_2) & \tau(l_1) \end{bmatrix} = \begin{bmatrix} k_1 + \phi k_2 & k_3 + \phi k_4 \\ \gamma(k_3 + \phi_1 k_4) & k_1 + \phi_1 k_2 \end{bmatrix} \tag{20}$$

where $\phi_1 = \tau(\phi) = \frac{1-\sqrt{5}}{2}$, $k_1, \ldots, k_4 \in \mathbb{K}$, $l_1 = k_1 + \phi k_2 \in \mathbb{L}$ and $l_2 = k_3 + \phi k_4 \in \mathbb{L}$.

The PAM symbols are carved from $\mathbb{Z}$. In what follows, we restrict $\gamma, k_1, \ldots, k_4$ to be belong to $\mathcal{O}_\mathbb{K}$ (the ring of integers of $\mathbb{K}$). The purpose of the construction is to assure that the matrices C_0 are invertible (except for the all-zero matrix). This is equivalent to saying that $\mathcal{A}$ must be a division algebra. It is well known [11] that this can be achieved if γ verifies the condition that there is no element in $\mathbb{L}$ whose norm is equal to γ.

We will see in what follows that performing the construction in $\mathcal{O}_\mathbb{K}$ rather than $\mathbb{K}$ and restricting γ to belong to $\mathcal{O}_\mathbb{K}$ results in a code that has a non-vanishing determinant [15], [16]. This property results in a code that achieves the diversity-multiplexing tradeoff of the underlying channel [10], [17].

Similar to [10], each sub-matrix C_k in eq. (17) is chosen to have the following structure:

$$\begin{aligned} C_k &= D\sigma^{k-1}(\lambda C_0) & (21)\\ &= \text{diag}\left((1+\phi^2)^{-\frac{1}{2}} \quad (1+\phi_1^2)^{-\frac{1}{2}}\right)\sigma^{k-1}(\lambda C_0) & (22)\end{aligned}$$

where the matrix D is introduced for normalization purposes. On the other hand, multiplying by λ limits the construction in a lattice of points whose volume is equal to 1. This can be viewed as a normalization process, and in some situations, it results in a transmitted constellation that is a rotation of the original signal set.

When K is odd, we fix $\lambda = \alpha \in \mathbb{K}$. Consider the ideal $I = \alpha\mathcal{O}_\mathbb{K}$, the volume of its generated lattice $\Lambda(I)$ must verify:

$$\text{vol}(\Lambda(I)) = \text{N}_{\mathbb{K}/\mathbb{Q}}(\alpha)\sqrt{d_{\mathbb{K}/\mathbb{Q}}} = 1 \tag{23}$$

where $d_{\mathbb{K}/\mathbb{Q}}$ is the discriminant of $\mathbb{K}$. When K is even, we fix $\lambda = \sqrt{\alpha}$. α is a totally positive algebraic element ($\sigma^k(\alpha) > 0$ for $k = 0, ..., K-1$) verifying $\text{N}_{\mathbb{K}/\mathbb{Q}}(\alpha)d_{\mathbb{K}/\mathbb{Q}} = 1$. In both cases

$$\text{N}_{\mathbb{K}/\mathbb{Q}}(\lambda) = \frac{1}{\sqrt{d_{\mathbb{K}/\mathbb{Q}}}} \tag{24}$$

Since $\mathbb{K}$ can be viewed as a K-dimensional vector space over $\mathbb{Q}$, $4K$ symbols can be included in each sub-matrix C_k resulting in a full rate code.

From eq. (16) and eq. (24), the determinant of C can be

expressed as:

$$\frac{\det(C)}{\det(D)^K} = \prod_{k=1}^{K} \det(\sigma^{k-1}(\lambda C_0)) = \prod_{k=1}^{K} \sigma^{k-1}(\det(\lambda C_0)) \tag{25}$$

$$= \mathrm{N}_{\mathbb{K}/\mathbb{Q}}(\lambda^2)\mathrm{N}_{\mathbb{L}/\mathbb{F}}(\underbrace{\mathrm{N}_{\mathbb{L}/\mathbb{K}}(k_1+\phi k_2)}_{\triangleq x} - \gamma \underbrace{\mathrm{N}_{\mathbb{L}/\mathbb{K}}(k_3+\phi k_4)}_{\triangleq y}) \tag{26}$$

$$= d_{\mathbb{K}/\mathbb{Q}}^{-1}\mathrm{N}_{\mathbb{L}/\mathbb{F}}(x-\gamma y) \tag{27}$$

Since there is no element in $\mathbb{L}$ whose norm is equal to γ, we obtain $x-\gamma y \neq 0$. Furthermore, $x-\gamma y \in \mathcal{O}_{\mathbb{K}}$ since $x, y, \gamma \in \mathcal{O}_{\mathbb{K}}$. Therefore, the minimum of the absolute value of eq. (27) is equal to $d_{\mathbb{K}/\mathbb{Q}}^{-1}$. As a conclusion, the minimum determinant of C is given by:

$$\delta_{min} = \min_{C \neq \mathbf{0}_{2K\times 2K}} |\det(C)| = \det(D)^K d_{\mathbb{K}/\mathbb{Q}}^{-1} \tag{28}$$

$$= (d_{\mathbb{F}/\mathbb{Q}})^{-\frac{K}{2}} d_{\mathbb{K}/\mathbb{Q}}^{-1} = (d_{\mathbb{L}/\mathbb{Q}})^{-\frac{1}{2}} > 0 \tag{29}$$

where $d_{\mathbb{L}/\mathbb{Q}}$ is the absolute discriminant of $\mathbb{L}$. Therefore, C achieves full diversity with a non-vanishing determinant that is independent from the size of the transmitted constellation.

From eq. (20), the matrix λC_0 can be expressed in an equivalent manner as:

$$\lambda C_0 = \sum_{i=0}^{1} \mathrm{diag}\left(\mathcal{R}\left[\begin{array}{ccc} a_{2iK+1} & \cdots & a_{2(i+1)K}\end{array}\right]^T\right)\Omega^i \tag{30}$$

$$R = \left[\begin{array}{cc} 1 & \phi \\ 1 & \phi_1 \end{array}\right] \otimes \mathcal{M} \quad ; \quad \Omega = \left[\begin{array}{cc} 0 & 1 \\ \gamma & 0 \end{array}\right] \tag{31}$$

$$\mathcal{M} = \left[\begin{array}{cccc} 1 & \theta & \cdots & \theta^{K-1}\end{array}\right] \tag{32}$$

where $a_1, ..., a_{4K}$ are the PAM information symbols.

In the same way, $\mathcal{M}$ can be calculated from any other unitary orthonormal basis $\{\sigma^k(v)\}_{k=0}^{K-1}$:

$$\mathcal{M} = \left[\begin{array}{cccc} v & \sigma(v) & \cdots & \sigma^{K-1}(v)\end{array}\right] \tag{33}$$

1) Information Losses: Designate by Φ the $4K\times 4K$ matrix that verifies the following relation:

$$\mathrm{vec}\,(C') \triangleq \mathrm{vec}\left(\left[C_1^T \ \cdots \ C_K^T\right]^T\right) = \Phi[a_1 \ \cdots \ a_{4K}]^T \tag{34}$$

In other words, C' is the vertical concatenation of the 2×2 matrices $C_1, \ldots, C_K$ given in eq. (21). In this case, Φ determines the linear dependence between the encoded symbols and the information symbols $a_1, \ldots, a_{4K}$.

From eq. (22), it is straight-forward to verify that the matrix Φ is given by:

$$\Phi = \left[\begin{array}{cc} \Phi_1^T & \Phi_2^T\end{array}\right]^T \tag{35}$$

$$\Phi_i = \left[\begin{array}{cccc} \Phi_{i,0}^T & \cdots & \sigma^{K-1}(\Phi_{i,0}^T)\end{array}\right]^T \quad ; \quad i=1,2 \tag{36}$$

$$\Phi_{1,0} = D\left[\begin{array}{cccc} \mathcal{M} & \phi\mathcal{M} & \mathbf{0}_{1\times K} & \mathbf{0}_{1\times K} \\ \mathbf{0}_{1\times K} & \mathbf{0}_{1\times K} & \gamma\mathcal{M} & \gamma\phi_1\mathcal{M}\end{array}\right] \tag{37}$$

$$\Phi_{2,0} = D\left[\begin{array}{cccc} \mathbf{0}_{1\times K} & \mathbf{0}_{1\times K} & \mathcal{M} & \phi\mathcal{M} \\ \mathcal{M} & \phi_1\mathcal{M} & \mathbf{0}_{1\times K} & \mathbf{0}_{1\times K}\end{array}\right] \tag{38}$$

where ϕ and ϕ_1 are the golden number and its conjugate respectively. D is the diagonal matrix defined in eq. (22) and $\mathcal{M}$ is given in eq. (33).

According to the definition given in [18], the diversity scheme is information-lossless if Φ is unitary. Considering the second row of $\Phi_{1,0}$, Φ can be unitary only when $\gamma^2 = 1$ since $\mathcal{M}\mathcal{M}^T = 1$. Therefore, totally-real information lossless codes can be obtained uniquely from $\gamma = \pm 1$. It can be directly seen that $\gamma = 1$ is not a feasible choice since it is always a norm in $\mathbb{L}$. In the same way we can show that we can not choose $\gamma = -1$. In fact, the first row of $\Phi_{1,0}$ is orthogonal to the second row of $\Phi_{2,0}$ if $\mathrm{N}_{\mathbb{F}/\mathbb{Q}}(\phi) = -1$ implying that $\mathbb{F}$ (and consequently $\mathbb{L}$) contains elements whose norms are equal to -1. Therefore, Φ is unitary implies that $\gamma = -1$ does not result in a division algebra. This shows the nonexistence of totally-real information-lossless codes based on cyclic division algebras.

2) Energy Balancing and Shaping: When $|\gamma| \neq 1$, the energy can be distributed in a more balanced way among the relays and symbol durations resulting in better performance [15]. Equation (20) can be expressed in an equivalent way as:

$$\lambda C_0 = c(\gamma)\lambda\left[\begin{array}{cc} k_1+\phi k_2 & \mathrm{sgn}(\gamma)|\gamma|^{\frac{1}{2}}(k_3+\phi k_4) \\ |\gamma|^{\frac{1}{2}}(k_3+\phi_1 k_4) & k_1+\phi_1 k_2\end{array}\right] \tag{39}$$

where $c(\gamma)^2 = \frac{2}{1+|\gamma|}$ is a normalization factor insuring the same transmitted energy as in uncoded systems. In this case, when γ is totally positive, eq. (29) becomes:

$$\delta_{min} = \frac{2^K}{\mathrm{N}_{\mathbb{K}/\mathbb{Q}}(1+\gamma)}(d_{\mathbb{L}/\mathbb{Q}})^{-\frac{1}{2}} \tag{40}$$

When it is possible to choose $\gamma \in \mathbb{Z}^+$, multiplying by the conjugates of λ results in a transmitted constellation that is a rotation of the original PAM signal set on each layer of the codeword. Let $k_i' = \gamma_i' k_i$ for $i = 1, \ldots, 4$ where $\gamma_i' = 1$ for $i = 1, 2$ and $\gamma_i' = \gamma^{\frac{1}{2}}$ for $i = 3, 4$. Since $\sigma^k(\gamma_i') = \gamma_i'$ for $k = 0, \ldots, K-1$, we have the following relation (for $i = 1, \ldots, 4$):

$$\left[k_i' \ \cdots \ \sigma^{K-1}(k_i')\right]^T = \gamma_i' \Gamma \left[a_{(i-1)K+1} \ \cdots \ a_{iK}\right]^T \tag{41}$$

where Γ is a $K\times K$ matrix whose k-th row is given by $\Gamma_k = \sigma^{k-1}(\mathcal{M})$ where $\mathcal{M}$ is given in eq. (33). Moreover, $\Gamma\Gamma^T = I_K$ which follows from eq. (24) and from the choice of an orthonormal basis resulting in a simple rotation of the PAM constellation. More precisely, the symbols contained in the conjugates of k_1 and k_2 are a simple rotation of the original information symbols. While the symbols contained in the conjugates of k_3 and k_4 are an amplified version of this same rotation. When γ is not a positive integer, eq. (41) does no hold for $i = 3, 4$ and shaping losses are introduced on the symbols contained in the conjugates of k_3 and k_4.

As a conclusion, the construction procedure consists of the correct choice of $\mathbb{K}$, a "non-norm" element $\gamma \in \mathcal{O}_{\mathbb{K}}$ and of an algebraic element α such that $\lambda = \alpha$ (resp. $\sqrt{\alpha}$) when K is odd (resp. even). Moreover, if the basis $\{\lambda\theta^k\}_{k=0}^{K-1}$ is not unitary, an appropriate basis transformation must be performed before applying eq. (31) and eq. (33). In what follows, we outline the construction procedure for $K = 1, \ldots, 5$.

- *1 relay*: In this case, we can choose C to be the totally real 2×2 code proposed in [3]:

$$C = \begin{bmatrix} (a_1 + \phi a_2) & \sqrt{2}(a_3 + \phi a_4) \\ \sqrt{2}(a_3 + \phi_1 a_4) & (a_1 + \phi_1 a_2) \end{bmatrix} \quad (42)$$

  where $a_1, ..., a_4$ are the information symbols. Using KANT software [19], we find that the we can choose $\gamma = 2$ since the ideal $2\mathcal{O}_{\mathbb{F}}$ is prime. From eq. (40), $\delta_{min} = \frac{2}{3} d_{\mathbb{F}/\mathbb{Q}}^{-\frac{1}{2}}$ with $d_{\mathbb{F}/\mathbb{Q}} = 5$ being the discriminant of $\mathbb{F} = \mathbb{Q}(\phi)$.
- *2 relays*: In this case, we choose $\mathbb{K} = \mathbb{Q}(\theta)$ with $\theta = 1 + \sqrt{2}$ and $d_{\mathbb{K}/\mathbb{Q}} = 2^3$. The choice $\lambda = \frac{\sqrt{3-\theta}}{2}$ verifies eq. (24) resulting in no shaping losses on the symbols contained in the conjugates of k_1 and k_2 as explained earlier. Moreover, λ and its conjugate are both real since $3 - \theta > 0$ and $3 - \theta_1 > 0$ where $\theta_1 = \sigma(\theta) = 1 - \sqrt{2}$. The rotation matrix $\mathcal{R}$ in eq. (31) can be calculated from $\mathcal{M} = \lambda[1 \quad \theta]$ since the basis $\{\lambda, \lambda\theta\}$ is unitary. In order to have a division algebra, we choose $\gamma = 1 + \theta$ since the ideal $\gamma\mathcal{O}_{\mathbb{L}}$ is prime implying that there is no element in $\mathbb{L}$ whose norm is equal to γ. Moreover, γ and $\sigma(\gamma)$ are both positive resulting in a minimum determinant that verifies eq. (40) (more precisely, $\delta_{min} = \frac{1}{70}$).
- *3 and 5 relays*: For $K = 3, 5$, the construction is performed in the field $\mathbb{Q}(2\cos(\frac{2\pi}{N}), \phi)$ where N verifies $\varphi(N) = 2K$ where $\varphi(.)$ is Euler's function ($N = 7, 11$ for $K = 3, 5$ respectively). $\sigma^k(\theta) = 2\cos(\frac{2\pi(k+1)}{N})$ for $k = 0, ..., K-1$. In both cases, we can choose $\gamma = 2$ since the ideals $2\mathcal{O}_{\mathbb{L}}$ are prime. The rotation matrix in eq. (31) can be constructed from eq. (33) by fixing: $7v = -2+2\theta+3\theta^2$ for $K = 3$ and $11v = 4+2\theta+2\theta^2-\theta^3$ for $K = 5$ [3], [20].
- *4 relays*: We fix $\mathbb{L} = \mathbb{Q}(\theta, \phi)$ with $\theta = 2\cos(\frac{2\pi}{16})$ and $d_{\mathbb{K}/\mathbb{Q}} = 2^{11}$. Using KANT software [19], we find that the prime factorization of the ideal $2O_{\mathbb{K}}$ is given by:

$$2O_{\mathbb{K}} = (\theta O_{\mathbb{K}})^4 \quad (43)$$

  Choosing $\alpha = \theta/8$ verifies eq. (24) since $\mathrm{N}_{\mathbb{K}/\mathbb{Q}}(\alpha) = \frac{1}{d_{\mathbb{K}/\mathbb{Q}}}$, but a problem arises since the second and third conjugates of α are negative. Using KANT, we find the unit $e = 1-\theta^2+\theta^3$ whose conjugates have the same sign as those of α and whose norm is equal to 1. Therefore, choosing $\alpha = \theta e/8 = (-2 + \theta + 4\theta^2 - \theta^3)/8$ results in a totally positive algebraic number such that $\lambda = \sqrt{\alpha}$ verifies eq. (24).
  The basis $\{\sqrt{\alpha}\theta^k\}_{k=0}^{K-1}$ is not orthogonal. Applying the LLL reduction on the Gramm matrix corresponding to the previous basis, we obtain the new basis $\left\{\sqrt{\sigma^n(2 + 3\theta - \theta^3)/8}\right\}_{n=0}^{3}$. Equation (33) can be calculated from the preceding basis. The element $\gamma = \theta$ results in a full diversity code since its generated ideal is prime.

3) Error Balancing: Since $|\gamma| \neq 1$, the transmitted energy is not evenly distributed among the information symbols of the codewords presented in eq. (39). Consider for example the k-th cooperation block with $|\sigma^{k-1}(\gamma)| > 1$. In this case, k_1 and k_2 (and therefore the symbols $a_1 \cdots a_{2K}$) are more vulnerable to error events since the biggest fraction of the transmitted energy is dedicated for the transmission of k_3 and k_4 (which are combinations of $a_{2K+1} \cdots a_{4K}$). However, we can take advantage of the fact that each symbol is conveyed by N_f pulses to introduce error balancing between the components of the information vector.

From eq. (21), instead of transmitting $C_k \otimes 1_{1\times N_f}$ in the k-th cooperation period, we transmit:

$$C_{k,bal} = \begin{bmatrix} C_k & C_k^{'} \end{bmatrix} \otimes 1_{1\times N_f/2} \quad (44)$$

where $C_k^{'}$ is obtained in the same way as C_k in eq. (21) by applying a cyclic permutation of order $2K$ on the information symbols. In what follows, "energy" balancing (Section III-A.2) is applied systematically in all cases, while the subscript "bal" will be reserved for error balancing.

B. Inter Pulse Coding (IPC)

In this case, the spreading vectors B_1 and B_2 from eq. (12) are chosen to be orthogonal to each other. It is worth noting that IPC is equivalent to the non-orthogonal AF scheme [9] even though the source and the relays are using low-dimensional orthogonal vectors during each cooperation interval. In fact, the multiple access scheme is controlled by the TH sequence which is common to the source and all its cooperating relays. If there is another source transmitting at the same moment, its corresponding relays can use the same vectors B_1 and B_2.

From eq. (11), combining the decision variables corresponding to the different pulses of the same symbol duration is equivalent to calculating:

$$Y\left(I_{KN_s} \otimes B^T\right) = \tilde{H}A\left(I_{KN_s} \otimes B^T\right) + N \quad (45)$$
$$= N_f \tilde{H} F + N \quad (46)$$

where B is a $2 \times N_f$ matrix given by $B = [B_1^T \quad B_2^T]^T$ and the noise term is always white. The matrix F can be expressed as:

$$F = \mathrm{diag}\left(\begin{bmatrix} \mathcal{A}_{1,1} \otimes e_1 \\ \mathcal{A}_{1,2} \otimes e_2 \end{bmatrix} \quad \cdots \quad \begin{bmatrix} \mathcal{A}_{K,1} \otimes e_1 \\ \mathcal{A}_{K,2} \otimes e_2 \end{bmatrix} \right) \quad (47)$$

where e_i is the i-th row of the 2×2 identity matrix. Since the dimensions of F are equal to $(2K, 2KN_s)$, there is no benefit in choosing $N_s > 1$, therefore we fix $N_s = 1$. In this case, F is a $2K \times 2K$ diagonal matrix. Therefore any full diversity rotation [20], [21] of the $2K$ information symbols is sufficient for achieving full diversity.

With respect to the ISC in Section III-A, IPC presents the advantage of lower decoding delays and lower peak to average power ratios (PAPR). Moreover, the decoding complexity is lower since each codeword contains $2K$ symbols rather than $4K$ symbols as in the case of ISC. However, unlike ISC, IPC can not be applied in the absence of pulse repetitions. In other words, IPC can be applied when at least $N_f = 2$ pulses are used to convey each symbol.

IV. Distributed ST codes with PPM-PAM constellations

For M-PPM-M'-PAM that are M-dimensional constellations, the codeword C_k transmitted by the source and the k-th relay during the second half of the k-th cooperation period must be a $2M \times 2$ matrix (rather than a 2×2 matrix as with PAM). We propose two solutions for the construction of $C_1, \ldots, C_K$ (and consequently the codeword C transmitted by the source and the K relays as in eq. (16)). The first solution consists of extending the codes proposed for PAM to M-dimensional constellations. The second solution consists of proposing new encoding schemes that are exclusive to M-dimensional constellations. This family of codes (that can not be applied with PAM) will be referred to as the PPM-PAM-specific code.

A. Extension of ISC and IPC to PPM-PAM

We propose to keep the same structure for the matrix C_0 given in eq. (39). In this case, the scalars $k_1, \ldots, k_4$ will become M-dimensional vectors carved from $\mathcal{O}_{\mathbb{K}}^M$ since the information symbols are now represented by M-dimensional vectors. The scalars λ and γ keep the same values as with PAM.

On the other hand, the new dimensionality of C_0 must be taken into account (C_0 is now a $2M \times 2$ matrix) and the normalization introduced in eq. (22) will be expressed as:

$$C_k = \text{diag}\left[(1+\phi^2)^{-\frac{1}{2}} 1_{1\times M} \quad (1+\phi_1^2)^{-\frac{1}{2}} 1_{1\times M}\right] \sigma^{k-1}(\lambda C_0) \tag{48}$$

ISC and IPC achieve full diversity with all constellations carved from $\mathbb{Z}$ since eq. (29) is calculated over all non-zero codewords. Therefore, the characteristics of the above codes do not change when they are applied with M-PPM-M'-PAM constellations. In particular, ISC and IPC continue to achieve full rate and full diversity. Moreover, the coding gain does not vanish when increasing the values of M and M'.

B. PPM-PAM-Specific Codes

The PPM-PAM-specific code takes a form similar to eq. (48), but now C_0 is given by:

$$C_0 = \begin{bmatrix} k_1 + \phi k_2 & k_3 + \phi k_4 \\ \Omega(k_3 + \phi_1 k_4) & k_1 + \phi_1 k_2 \end{bmatrix} \tag{49}$$

where $k_i = \sum_{j=0}^{K-1} A_{(i-1)K+j+1}\theta^j$ for $i = 1, \ldots, 4$ with $A_1, \ldots, A_{4K}$ being the M-dimensional vector representations of the information symbols. Each vector contains exactly $M-1$ zeros and one non-zero component that belongs to the M'-PAM constellation. It is this particular structure of $A_1, \ldots, A_{4K}$ that renders this construction fully diverse with PPM-PAM.

Unlike the codes based on cyclic division algebras (ISC and IPC) where full diversity is achieved by multiplying the lower triangular part of C_0 by the non-norm element γ (as in eq. (20)), the PPM-PAM-specific codes are based on introducing the $M \times M$ cyclic permutation matrix Ω given by:

$$\Omega = \begin{bmatrix} \mathbf{0}_{1\times(M-1)} & 1 \\ I_{M-1} & \mathbf{0}_{(M-1)\times 1} \end{bmatrix} \tag{50}$$

Denote by $\Delta C(X,Y)$ the difference between two codewords:

$$\Delta C(X,Y) = C_0 - C_0' = \begin{bmatrix} X & Y \\ \Omega\tau(Y) & \tau(X) \end{bmatrix} \tag{51}$$

where the M-dimensional vectors X and Y belong to the set $\mathcal{D}$ given by:

$$\mathcal{D} = \{\sum_{i=1}^{2K}(A_i - A_i')t_i \;\; ; \;\; A_1, \ldots, A_{2K}, A_1', \ldots, A_{2K}' \in \mathcal{C}\} \tag{52}$$

where $\mathcal{D} \subset \mathcal{O}_{\mathbb{L}}^M$, $\{t_i\}_{i=1}^{2K} = \{1, \theta, ..., \theta^{K-1}, \phi, \phi\theta, ..., \phi\theta^{K-1}\}$ and $\mathcal{C}$ stands for the M-PPM-M'-PAM constellation given in eq. (13).

With respect to the set $\{t_i\}_{i=1}^{2K}$ that forms a basis over $\mathbb{Q}$, the m-th component of X is represented by $2K$ coordinates for $m = 1, \ldots, M$. Vectors of $\mathcal{D}$ are linear combinations of $4K$ columns of the identity matrix I_M. They have the property that a maximum number of two components can have their i-th coordinates different from 0 for $i = 1, \ldots, 2K$.

In order to achieve a full diversity order, the rank of $\Delta C(X,Y)$ must be equal to 2 for all values of $(X,Y) \in \mathcal{D}^2 - \{(\mathbf{0}_{M\times 1}, \mathbf{0}_{M\times 1})\}$. From eq. (51), $\text{rank}(\Delta C(X,Y)) < 2$ implies that there exists a non-zero constant $l \in \mathbb{L}$ such that: $Y = lX$ and $\tau(X) = l\Omega\tau(Y)$. Solving these equation, we obtain that X and Y must verify:

$$\Omega X = \frac{1}{\text{N}_{\mathbb{L}/\mathbb{K}}(l)} X \tag{53}$$

where $\text{N}_{\mathbb{L}/\mathbb{K}}(l) \in \mathbb{K}^*$ since $l \neq 0$.

The eigenvalues of Ω are equal to ω^m for $m = 0, ..., M-1$ where $\omega = \text{e}^{\frac{2\pi i}{M}}$ is the M-th root of unity. Equation (53) shows that X (and Y) is an eigenvector of Ω. Moreover, being real valued, X must be associated with a real eigenvalue of Ω.

When M is odd, the real vectors verifying eq. (53) are the real-multiples of $1_{M\times 1}$. When M is even, the real solutions of eq. (53) are the real-multiples of $1_{M\times 1}$ and $[1\ -1 \cdots 1\ -1]^T$. Therefore in both cases, when $X \in \mathcal{O}_{\mathbb{L}}^M$, $\exists t \in \{1, ..., 2K\}$ such that the t-th coordinates of the M components of X are different from 0. This shows that $X \notin \mathcal{D}$ for $M > 2$ since, from eq. (52), only two vectors A_t and A_t' can result in non-zero t-th coordinates. Therefore, the vectors that result in rank deficient codewords do not belong to $\mathcal{D}$ for $M > 2$. Moreover, since the proof is independent from M', the code achieves full diversity with $M > 2$, $\forall\ M'$.

As in the previous section, the basis $\lambda\{1, ..., \theta^{K-1}\}$ can be replaced by an orthonormal basis $\{\sigma^k(v)\}_{k=0}^{K-1}$. As in eq. (34), consider the matrix Φ obtained from writing $\text{vec}(C') = \Phi[A_1^T \cdots A_{4K}^T]^T$. It is easy to show that choosing Ω to be unitary and the basis $\{\sigma^k(v)\}$ to be orthonormal results in a unitary matrix Φ. Therefore, the code is information lossless [18]. In an equivalent manner, it introduces no shaping losses according to the definition given in [12].

1) Coding Gain:

Designate by $\delta_{M,M'}$ the coding gain of a distributed ST code when associated with M-PPM-M'-PAM. Unlike the codes constructed from cyclic division algebras that have a non-vanishing coding gain (ISC and IPC and their extensions to

PPM-PAM), for the PPM-PAM specific codes $\delta_{M,M'}$ may decrease with M'.

On the other, for a given value of M', $\delta_{M,M'}$ increases with M since new dimensions are added to the signal set. Therefore, we can argue that for $M >> 1$, $\delta_{M,M'}$ will keep the same value for all values of M' (this value will be the highest achievable coding gain). Instead of achieving a non-vanishing coding gain for infinitely large values of M, we can prove that this can happen for finite values of M. Formally speaking, we can prove the following:

Proposition: For a cooperative system with K relays, combining eq. (49) and eq. (50) permits to achieve a non-vanishing coding gain with M-PPM-M'-PAM constellations for $M \geq 4K+1$ and for all values of K.

Proof: The proof is provided in the appendix.

When $M \geq 4K+1$, the PPM-PAM-specific coding becomes "perfect" according to the definition given in [12]. In particular, this family of codes will achieve full rate and full diversity with a non-vanishing coding gain while being information-lossless and shape preserving.

C. Comparing the PPM-PAM Codes

The PPM-PAM-specific code given in Section IV-B has the same decoding complexity as ISC and balanced-ISC given in Section IV-A ($4K$ symbols per codeword). However ISC and balanced-ISC have higher PAPR. This follows from introducing the scalar γ in eq. (39) whose magnitude is different from 1.

On the other hand, for very high data rate systems that do not employ any pulse repetitions, balanced-ISC and IPC can not be applied. We next compare ISC with the modulation-specific code (MSC) in the two cases where $M < 4K+1$ and $M \geq 4K+1$.

For $M < 4K+1$, comparing MSC with ISC, we notice that MSC is information lossless at the expense of a coding gain that can decrease with the size of the PAM constellation (M'). On the other hand, ISC has a non-vanishing determinant (NVD) but it is not information-lossless.

For Rayleigh fading channels, having a NVD is a very interesting feature since it results in codes that achieve the diversity-multiplexing (D-MG) tradeoff [10], [17]. In this context, the NVD property can be more interesting than the shaping property. For UWB communications, we argue that the shaping constraint can be more important than the NVD constraint for the following reasons. First, the D-MG tradeoff is considered over Rayleigh fading channels while the propagation of UWB signals is subject to lognormal fading [5]. For these channels, and even for single-antenna situations, it is easy to find that the slope of the outage probability curves tends to infinity for large SNRs implying an ambiguity on the D-MG tradeoff with lognormal fading. On the other hand, the spectral efficiency of M-PPM-M'-PAM can be increased by extending the constellation in the position domain (increasing M) rather than the amplitude domain (increasing M'). As we've seen earlier, this extension does not reduce the coding gain.

For $M \geq 4K+1$, the superiority of MSC is evident since it is information lossless and it has a NVD. Moreover, it is straightforward to prove that the coding gain of MSC is higher since the normalization factor $c(\gamma)$ introduced in eq. (39) reduces the coding gain of ISC.

V. Simulations and results

In this section, we present simulations and comparisons in order to validate the designed codes. The random channels between the different radio terminals are generated according to the channel model presented in [5]. In particular, we present simulations over CM1 and CM2 that correspond to line-of-sight (LOS) and non-line-of-sight (NLOS) conditions respectively. We select the pulse shaper $w(t)$ to be the second derivative of the Gaussian function with a duration of 0.5 ns. The modulation delay is chosen as $\delta = 0.5$ ns. The number of pulses transmitted per symbol has no impact on the performance in the absence of interference. It is chosen to be a multiple of 2 to render error balancing and IPC possible. The transmitted energy is chosen to be equally distributed among the two halves of the cooperation period ($\beta_1 = \beta_2$ in eq. (8)). At the destination, the sphere decoder [22] is used for detection. In the first set of simulations, we suppose that the different propagation delays are compensated at the destination.

The objective of the first simulation setup is to compare the distributed codes with PAM. Namely, we perform comparisons between ISC in eq. (39), balanced-ISC in eq. (44) and IPC in Section III-B. In order to highlight the effect of the achieved diversity, we consider systems that do not have any energetic gain. In other words, we fix $\rho_k = \delta_k = 1$ in eq. (8). In this case the distances source-relay, relay-destination and source-destination are supposed to be the same.

Fig. 2 shows the performance on CM2 with 2 PAM. The relay and the destination are equipped with 5-fingers Rakes. The performance gain resulting from the proposed distributed ST codes is evident. Fig. 2 shows the importance of error balancing. The unbalanced ISC from eq. (42) shows poor performance especially at low signal to noise ratios since the performance is limited by the error events occurring on the less protected symbols a_1 and a_2. Using balanced-ISC from eq. (44) results in a gain of about 2.5 dB at a BER of 10^{-3}. IPC shows comparable performance with respect to balanced-ISC. The gap between the two codes results from the interleaving imposed by eq. (44) resulting in a better immunity against noise.

Fig. 3 shows the performance on CM2 with 2 PAM and a 5-finger Rake. Simulation results with $K = 2$ and $K = 4$ relays are presented. The reduced decoding complexity of IPC incurs a loss that is less than 1 dB with respect to balanced-ISC that shows the best performance. Similar results are obtained in Fig. 4 with 3 and 5 relays using a 1-finger Rake. Since the amplitude of the first arriving multi-path component can be very small in NLOS configurations [5], the noise events have a critical role in determining the system performance. This explains the relatively large gap between IPC and balanced-ISC.

Fig. 5 shows the performance on CM2 with multi-dimensional constellations. In particular the PPM-PAM extensions of ISC and balanced-ISC (Section IV-A) are compared

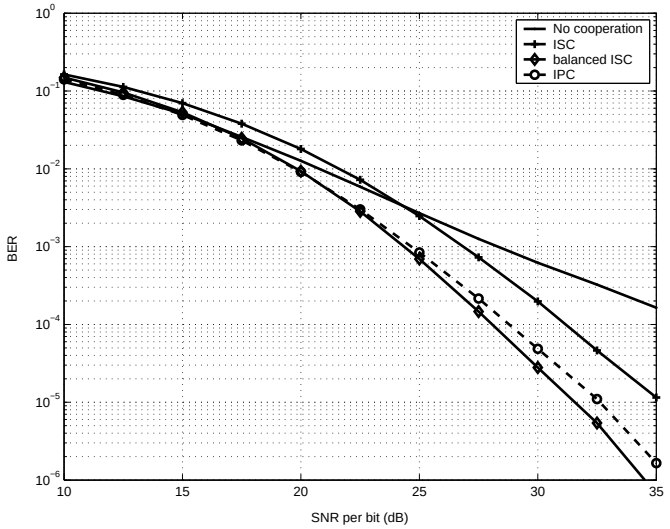

Fig. 2. Performance on CM2 with 1 relay, 2 PAM constellations and a 5-fingers Rake.

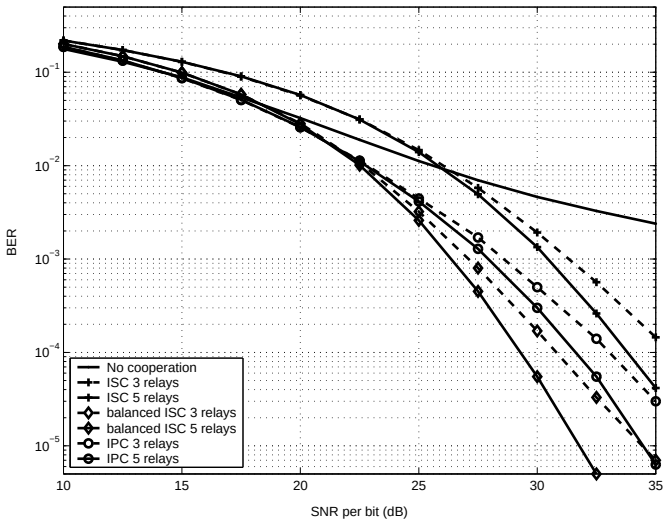

Fig. 4. Performance on CM2 with 2 PAM and 1-finger Rake using 3 and 5 relays.

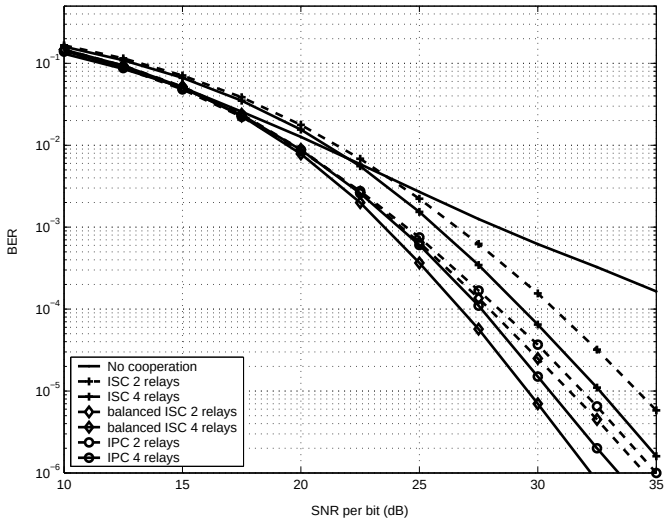

Fig. 3. Performance on CM2 with 2 PAM and 5-fingers Rake using 2 and 4 relays .

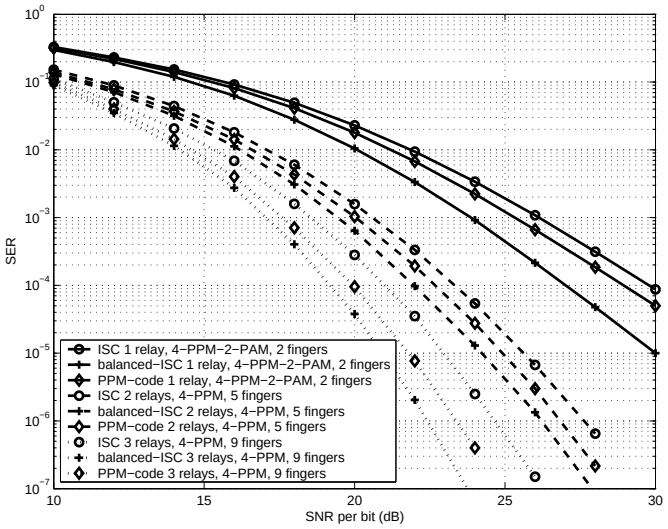

Fig. 5. Performance on CM2 with multi-dimensional constellations. 'PPM-code' corresponds to the code given in Section IV-B.

with the modulation-specific code (MSC) given in Section IV-B. Results show the interest of using MSC rather than the extension of codes constructed over infinite fields. MSC outperforms ISC and approaches the performance of balanced-ISC without performing any kind of intra-symbol coding. This shows the importance of using information-lossless codes.

In the second simulation setup, ρ_k and δ_k are determined from the relative positions of the terminals assuming free space propagation. The source and destination are separated by a distance of $d = 10$ m. The positions of the K relays are uniformly distributed in the surface determined from the intersection of the two circles whose radii are equal to d and centered at the source and the destination respectively. We compare the two cases where the relative propagation delays between the relays and destination are compensated or not. IPC is used with 2 PAM, one relay and a 4-finger Rake. Results shown in Fig. 6 show the performance losses that result in the case where the propagation delays between the relays and the destination are not compensated. CM1 is more vulnerable to this "misalignment".

In the third setup, simulations are performed over a realistic indoor channel. In this context, the site-specific channel modeling tools [13], [14] can be beneficial in simulating wireless networks in realistic indoor environments. These tools are based on "Ray-Tracing" and they take the geometry of the explored environment into consideration. The explored environment corresponds to a typical office building whose map is given in Fig. 7. The transmitted signal corresponds to a Gaussian pulse occupying the band $[3\ 5]$ GHz. The gain parameters ρ_k and δ_k in eq. (8) are determined explicitly from this model that determines the path loss associated with each multi-path component from a given transmitter to one of the four reference nodes. We consider the communication between the reference nodes "2" and "4" with one cooperating relay

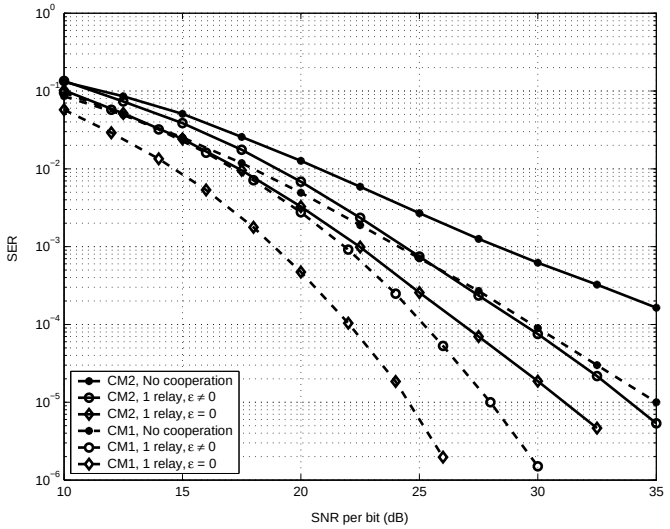

Fig. 6. Performance with 2 PAM and a 5-finger Rake in the cases where the different propagation delays are compensated or uncompensated.

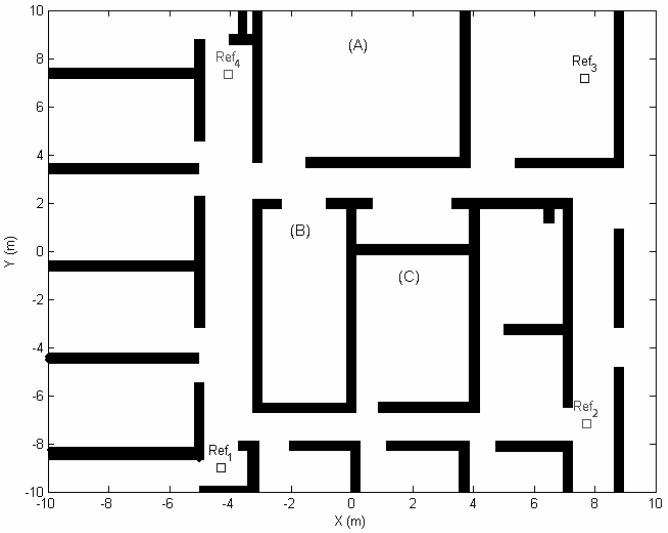

Fig. 7. Map of the studied environment.

that can occupy any position in the rooms (A), (B) and (C). Simulations of balanced-ISC with 4 PAM and a 4-finger Rake are shown in Fig. 8. The same simulations are repeated in Fig. 9 with 2 relays. Results show that in realistic indoor channels, important performance gains can be achieved depending on the relative positions of the source, destination and the relays. Moreover, a "bad" channel between the source and a relay can be more penalizing than a channel having the same quality between this relay and the destination.

VI. Conclusion

In this work, we have presented a general construction technique of distributed ST-TH-UWB codes for the NAF cooperation scheme. These totally-real codes are well suited for low complexity carrier-less UWB systems. The pulse repetitions intrinsic to TH-UWB systems were further exploited resulting in an enhanced performance and reduced decoding complexity. For PAM constellations, inter symbol coding associated with error balancing achieved the best performance while inter pulse coding achieved a comparable performance with reduced complexity and lower PAPR. For multi-dimensional hybrid PPM-PAM, a new construction based on permutations was shown to have the best performance among systems that do not employ any pulse repetitions. The proposed schemes result in important performance gains that can mitigate the problems related to the propagation properties of UWB signals. In an equivalent manner, the limited communication ranges of UWB systems can be significantly enhanced.

Appendix

The matrix $\Delta C_0(X,Y)$ given in eq. (51) can be written in a more explicit form as:

$$\Delta C_0(X,Y) = \begin{bmatrix} X_1 & \cdots & X_M & \tau(Y_{\pi^{-1}(1)}) & \cdots & \tau(Y_{\pi^{-1}(M)}) \\ Y_1 & \cdots & Y_M & \tau(X_1) & \cdots & \tau(X_M) \end{bmatrix}^T \quad (54)$$

where $\pi^k(.)$ stands for the cyclic permutation of order k given by:

$$\pi^k(m) = (m+k-1) \mod M+1 \quad (55)$$

From $\Delta C_0(X,Y)$ we construct the matrix $\Delta C(X,Y)$ given by:

$$\Delta C(X,Y) = \text{diag}\left[\Delta C_0(X,Y) \quad \sigma(\Delta C_0(X,Y)) \quad \cdots \quad \sigma^{K-1}(\Delta C_0(X,Y))\right] \quad (56)$$

in other words $\Delta C(X,Y)$ stands for the difference between two codewords transmitted by the source and its K relays during the entire interval of cooperation.

In what follows, $\Delta C_0(X,Y)$ and $\Delta C(X,Y)$ will be referred to as ΔC_0 and ΔC respectively when there is no ambiguity. Moreover, we denote by $\Delta C_{0,i}$ the i-th row of ΔC_0.

ΔC_0 verifies the following relation for all values of M:

$$\det\left((\Delta C_0)^T \Delta C_0\right) = \sum_{i_1=1}^{2M} \sum_{i_2=i_1+1}^{2M} \left(\det\left(\left[(\Delta C_{0,i_1})^T \quad (\Delta C_{0,i_2})^T\right]^T\right)\right)^2 \quad (57)$$

From eq. (52), X and Y are linear combinations of $4K$ columns of I_M. Therefore, for $M \geq 4K+1$, X and Y each contain at least one zero component. Designate by $m \in \{1,\ldots,M\}$ the index of the component of X that is equal to zero, that is, $X_m = 0$.

Considering the m-th and the $(M+\pi(m))$-th rows of ΔC_0, we obtain:

$$\det\left((\Delta C_0)^T \Delta C_0\right) \geq \left(\det\left(\left[(\Delta C_{0,m})^T \quad (\Delta C_{0,M+\pi(m)})^T\right]^T\right)\right)^2 = \mathrm{N}_{\mathbb{L}/\mathbb{K}}\left(Y_m^2\right) \quad (58)$$

This implies that:

$$\det\left((\Delta C)^T \Delta C\right) \geq \mathrm{N}_{\mathbb{L}/\mathbb{Q}}\left(Y_m^2\right) \quad (59)$$

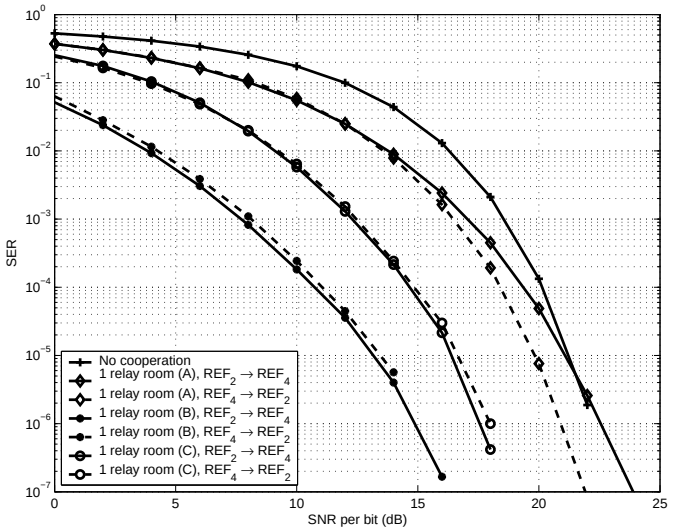

Fig. 8. Performance in the studied environment with 4 PAM, 4-fingers Rake and 1 relay. The relay can occupy any position in rooms (A), (B) and (C) and it participates in the communication between REF_2 and REF_4.

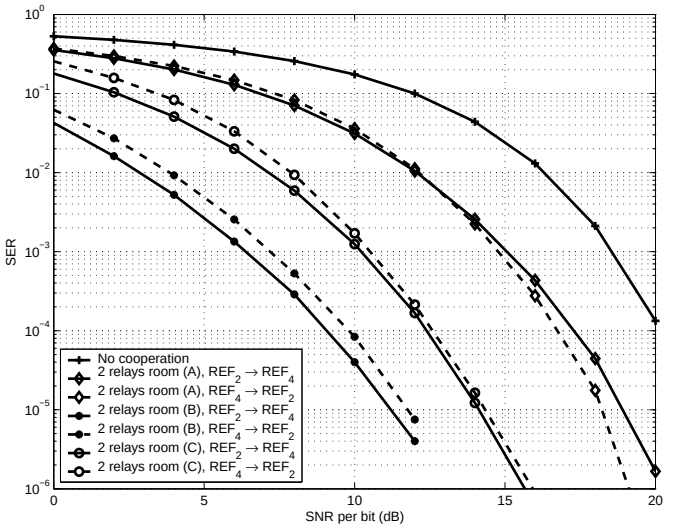

Fig. 9. Performance in the studied environment with 4 PAM, 4-fingers Rake and 2 relays. The relays can occupy any position in rooms (A), (B) and (C) and they participate in the communication between REF_2 and REF_4.

proving that $\det\left((\Delta C)^T \Delta C\right) \geq 1$ unless when $Y_m = 0$.

Now, considering the $\pi(m)$-th and the $(M+\pi(m))$-th rows of ΔC_0, we obtain:

$$\det\left((\Delta C_0)^T \Delta C_0\right) \geq$$
$$\left(\det\left(\left[(\Delta C_{0,\pi(m)})^T \quad (\Delta C_{0,M+\pi(m)})^T\right]^T\right)\right)^2 = \mathrm{N}_{\mathbb{L}/\mathbb{K}}(X^2_{\pi(m)})$$

implying that $\det\left((\Delta C)^T \Delta C\right) \geq \mathrm{N}_{\mathbb{L}/\mathbb{Q}}(X^2_{\pi(m)})$ and, consequently, $\det\left((\Delta C)^T \Delta C\right) \geq 1$ unless when $X_{\pi(m)} = 0$.

Starting the same procedure again with $\pi(m)$ rather than m, we can show by induction that $\det\left((\Delta C)^T \Delta C\right) \geq 1$ unless when $X_m = \cdots = X_{\pi^{M-1}(m)} = 0$ and $Y_m = \cdots = Y_{\pi^{M-1}(m)} = 0$. Since $\{m, \ldots, \pi^{M-1}(m)\}$ spans the entire set $\{1, \ldots, M\}$ for all values of m, this implies that $\det\left((\Delta C)^T \Delta C\right) \geq 1$ unless when $X = Y = \mathbf{0}_{M\times 1}$. Consequently, the considered code has a non-vanishing coding gain since $\det\left((\Delta C)^T \Delta C\right)$ (and consequently the minimum of this quantity taken over the entire constellation) is lower bounded by a non-zero number.

REFERENCES

[1] F. C. Commission, "First report and order, technical report FCC 02-48," www.fcc.gov., April 2002.

[2] L. Yang and G. B. Giannakis, "Analog space-time coding for multi-antenna ultra-wideband transmissions," *IEEE Trans. Commun.*, vol. 52, pp. 507–517, March 2004.

[3] C. Abou-Rjeily, N. Daniele, and J.-C. Belfiore, "Space time coding for multiuser ultra-wideband communications," *IEEE Trans. Commun.*, vol. 54, pp. 1960–1972, November 2006.

[4] L. Huaping, R. C. Qiu, and T. Zhi, "Error performance of pulse-based ultra-wideband MIMO systems over indoor wireless channels," *IEEE Trans. Wireless Commun.*, vol. 4, pp. 2939–2944, November 2005.

[5] J. Foerster, "Channel modeling sub-committee Report Final," Technical report IEEE 802.15-02/490, IEEE 802.15.3a Wireless Personal Area Networks, 2002.

[6] J. Keignart, C. Abou-Rjeily, C. Delaveaud, and N. Daniele, "UWB SIMO channel measurements and simulations," *IEEE Trans. Microwave Theory Tech.*, vol. 54, pp. 1812–1819, April 2006.

[7] J. Laneman and G. Wornell, "Distributed space time coded protocols for exploiting cooperative divesrity in wireless networks," *IEEE Trans. Inform. Theory*, vol. 49, no. 10, pp. 2415–2425, October 2003.

[8] J. Laneman, D. Tse, and G. Wornell, "Cooperative diversity in wireless networks: Efficient protocols and outage behavior," *IEEE Trans. Inform. Theory*, vol. 50, pp. 3062–3080, December 2004.

[9] K. Azarian, H. El Gamal, and P. Schinter, "On the achievable diversity-multiplexing tradeoffs in half-duplex cooperative channels," *IEEE Trans. Inform. Theory*, vol. 51, no. 12, pp. 4152–4172, December 2005.

[10] S. Yang and J.-C. Belfiore, "Optimal space-time codes for the MIMO amplify-and-forward cooperative channel," *IEEE Trans. Inform. Theory*, vol. 53, no. 2, pp. 647–663, February 2007.

[11] B. A. Sethuraman, B. S. Rajan, and V. Shashidhar, "Full-diversity, high rate space-time block codes from division algebras," *IEEE Trans. Inform. Theory*, vol. 49, pp. 2596–2616, October 2003.

[12] F. Oggier, G. Rekaya, J.-C. Belfiore, and E. Viterbo, "Perfect space time block codes," *IEEE Trans. Inform. Theory*, vol. 52, no. 9, pp. 3885 – 3902, September 2006.

[13] B. Uguen, E. Plouhinec, Y. Lostanlen, and G. Chassay, "A deterministic ultra wideband channel modeling," in *IEEE Conference on Ultra Wideband Systems and Technologies*, May 2002, pp. 1–5.

[14] F. Tchoffo-Talom, B. Uguen, E. Plouhinec, and G. Chassay, "A site-specific tool for UWB channel modeling," in *IEEE Conference on Ultra Wideband Systems and Technologies*, May 2004, pp. 18–21.

[15] J.-C. Belfiore and G. Rekaya, "Quaternionic lattices for space-time coding," in *Proceedings IEEE Information Theory Workshop*, vol. 2, April 2003, pp. 267–270.

[16] J.-C. Belfiore, G. Rekaya, and E. Viterbo, "The Golden code: a 2×2 full-rate space-time code with nonvanishing determinant," *IEEE Trans. Inform. Theory*, vol. 51, no. 4, pp. 1432–1436, April 2005.

[17] P. Elia, K. R. Kumar, S. A. Pawar, P. V. Kumar, and H. Lu, "Explicit, minimum-delay space-time codes achieving the diversity-multiplexing gain tradeoff," *IEEE Trans. Inform. Theory*, vol. 52, no. 9, pp. 3869–3884, September 2006.

[18] M. O. Damen, A. Tewfik, and J.-C. Belfiore, "A construction of a space-time code based on number theory," *IEEE Trans. Inform. Theory*, vol. 48, no. 3, pp. 753–760, March 2002.

[19] M. Daberkow, C. Fieker, J. Klners, M. Pohst, K. Roegner, and K. Wildanger, "Kant v4," *J. Symbolic Comp.*, vol. 24, 1997.

[20] E. Bayer, F. Oggier, and E. Viterbo, "New algebraic constructions of rotated $\mathbb{Z}^n$ lattice constellations for the Rayleigh fading channel," *IEEE Trans. Inform. Theory*, vol. 50, pp. 702–714, April 2004.

[21] E. Viterbo and J. J. Boutros, "Signal space diversity: a power- and bandwidth-efficient diversity technique for the Rayleigh fading channel," *IEEE Trans. Inform. Theory*, vol. 44, no. 4, pp. 1453–1467, July 1998.

[22] M. O. Damen, H. E. Gamal, and G. Caire, "On maximum-likelihood detection and the search for the closest lattice point," *IEEE Trans. Inform. Theory*, vol. 49, pp. 2389–2402, October 2003.